# TALOS Wave Energy Converter Power Output Prediction Analysis Based on a Machine Learning Approach

Yueqi Wu, Wanan Sheng, C. James Taylor, George Aggidis, Xiandong Ma*
School of Engineering, Lancaster University
Lancaster, United Kingdom

## ABSTRACT

**Wave energy shows potential to provide electricity in a renewable manner. The TALOS WEC (Wave Energy Converter) is a unique design with six PTO (Power Take-Off) elements to provide six Degrees of Freedom (DOFs). It is potentially able to harvest energy more efficiently than traditional single-DOF devices. As a step towards its optimisation and control, a power prediction model is developed, using the wave elevation and motions of the WEC to predict the power output of each PTO. The results show that using LSTM (Long-Short Term Memory) has a higher prediction accuracy than the other approaches considered.**

KEY WORDS: TALOS, WEC, Power Prediction, Machine Learning, LSTM.

## INTRODUCTION

Much research has been done on energy harvesting technologies over the past few decades, in part due to the incoming energy crisis. As a type of renewable energy, ocean waves provide significant energy via a sustainable and reliable approach. As a result, many different types of WECs have been designed and tested to produce clean and renewable energy (Li et al., 2012). Examples include Lancaster University's PS Frog (Taylor et al., 2002; McCabe et al., 2006), AquaBuOy (AquaBuOy, 2016), and Powerbuoy (Powerbuoy, 2016).

In general, WECs can be categorised as point absorbers, oscillating water columns, terminators, oscillating wave surge converters, attenuators, and submersed pressure differential devices (Aggidis and Taylor, 2017; Darwish and Aggidis, 2022). The majority of WECs are single-DOF devices, which means they could only extract energy from one direction of motion. Based on the single-DOF method, prototypes have been designed such as the Carnegie Wave Energy Limited prototypes (Wave Hub, 2016), the Archimedes Wave Swing (AWS Ocean, 2016), Oregon Limited's multi-resonant chamber (Orecon, 2009), and Salter's Duck (Salter, 1974). However, the kinetic power contained in the waves is in multiple directions. In hydrodynamic analysis, the waves have yaw, roll, and pitch motions in heave, surge, and sway axes, respectively. In total, there are six degrees of freedom in WECs that would be affected by the waves. Theoretically, if the device can extract energy from multiple DOFs, more energy can be thus generated.

Despite most designs being single-DOF, few multi-DOF WECs have been developed to date. One of the most famous designs is Pelamis, which is a snake shape device with several tubes that are connected by hydraulic rams. The electricity is generated from the hydraulic rams that connect the moving tubes. Pelamis prototypes have been deployed in Portugal and Scotland and fed electricity in national grids (Boyle and Duckers, 2012).

Compared with single-DOF devices, multi-DOF WECs have seen much less research and prototype design. Development of Pelamis, for example, was cancelled because the company went into administration after being unable to secure the level of additional funding required for the further development of their technology (Wave power firm Pelamis calls in administrators, 2014). NHP-WEC (Novel High-performance Wave Energy Converter) is an ongoing project that aims to design a novel multi-DOF point absorber style WEC, called TALOS, built as a 1/100th scale representation, with a solid outer hull containing all the moving parts. These include a ball mass and dampers (PTOs) that connect the ball and the hull, as shown in Fig. 1.

During the development of the prototype, ocean uncertainties threaten the reliability and stability of the ocean energy system, especially for WECs (Sanchez et al., 2018). Hence, it is necessary to forecast ocean wave energy to save construction and pilot project costs (Reikard et al., 2015). Prediction of WEC power output can bring the following benefits:

- Improve the design of the control system.
- Improve power management abilities.
- Improve the reliability of the condition monitoring system.

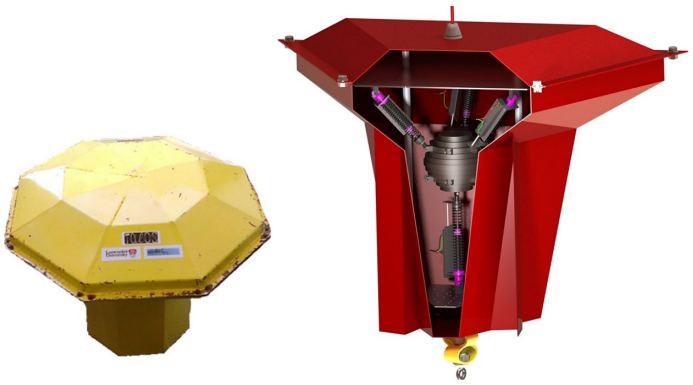

Fig. 1 TALOS I photograph (left) and TALOS II prototype diagram, with cut away section to show the internal PTO components (from Bhatt et al., 2016).

Machine learning algorithms, integral to the field of artificial intelligence (AI), are developed to recognize patterns in data, enabling predictive analytics and enhancing their performance through learning from experience. These algorithms are primarily categorised based on their learning approach and the nature of the data they are trained on.

Supervised learning algorithms are trained using data that is labelled, meaning each data point is associated with a known output. This type of learning is akin to a student learning under the guidance of a teacher, where the algorithm learns to map inputs to the given outputs (Cunningham and Delany, 2008). Linear Regression and Logistic Regression are examples of supervised learning algorithms, with the former used for continuous outcome prediction and the latter for categorical outcome prediction. Specific algorithms like Support Vector Regression (SVR), Artificial Neural Networks (ANN), and Regression Trees also play a significant role in machine learning. SVR is used in cases where the goal is to predict continuous values, but unlike traditional regression, it focuses on minimizing error margins and is particularly effective in high-dimensional spaces. ANNs, inspired by biological neural networks, consist of interconnected nodes or neurons and are particularly adept at processing complex patterns in large-scale data. They are widely used in image and speech recognition, among other applications. Regression Trees, a part of the decision tree algorithm family, are used for predicting continuous target variables. They split the data into subsets based on certain criteria, making them valuable for tasks that require a hierarchical, decision-making approach (Xiang et al., 2018).

Unsupervised learning, in contrast, deals with unlabelled data. The algorithms in this category aim to identify hidden patterns or intrinsic structures within the data. They are not provided with correct answers but must find the structure and relationships in the data on their own. K-Means Clustering and the Apriori algorithm are prime examples of unsupervised learning algorithms, used for clustering and association rule mining, respectively (Yürüşen, 2021).

Reinforcement learning is a distinct category where an agent learns to make decisions by performing actions within an environment. It is guided by feedback in the form of rewards or penalties. Q-Learning is a popular algorithm in this category, employed in scenarios where sequential decision-making is crucial under uncertain conditions (Arulkumaran, 2017).

Machine learning (ML) is becoming increasingly integral to industry. ML algorithms have been widely applied in various sectors, including, for example, the water turbine business, wind turbine efficiency analysis, and ship hull overload prediction. In the water industry, ML is utilized for water quality monitoring, leakage detection, and network optimization. Melbourne Water has employed a Python-based AI and ML system to significantly reduce energy costs in treatment plant pump-stations (Joseph, 2022). Sydney Water has developed 'Sewer Scout', a tool for accurately locating maintenance chambers and identifying sewer system defects. Additionally, ML applications in the wind energy sector include predictive maintenance and power generation optimization, enhancing operational efficiency and energy output. In the context of ship hull overload prediction, ML is employed to analyse structural integrity and predict potential failures, thus improving maritime safety and efficiency (Benbouzid, 2021).

In the realm of ocean energy, most existing research focuses on wave prediction. A notable study by Desouky and Abdelkhalik (2019) employs an ANN and NARX (nonlinear autoregressive network with exogenous inputs) for predicting wave surface elevation. Zhang et al. (2022) introduced a variational Bayesian machine learning method to predict wave elevation, uncertainty, and the predictable zone, demonstrating lower prediction errors compared to linear wave theory and deterministic machine learning approaches.

However, predicting the power output of WECs presents more complex challenges due to the intricate boundary condition equations involved. To address this, Mousavi et al. (2021) explored ML-based solutions as alternatives to traditional numerical methods. The adoption of genetic algorithms for creating prediction models using various wave periods, heights, and water depths has been investigated by Liu et al. (2020). Additionally, other ML methods such as reinforcement learning, K-means clustering, and Convolutional Neural Networks (CNNs) have been utilized for predicting electricity generation from WECs, as reported in studies by Zou et al. (2022), Wang (2020), and Ni et al. (2018).

In the quest to model the TALOS WEC, the integration of Kernel Principal Component Analysis (KPCA) with Long Short-Term Memory (LSTM) networks, alongside SVR, ANN, and Regression Trees, constitutes a robust, strategic algorithmic ensemble. SVR's prowess in tackling non-linear data is indispensable for modelling the intricate dynamics present in wave energy systems. ANN's are invaluable for their capacity to approximate complex and non-linear interdependencies that are characteristic of wave energy converters' behaviours. Regression Trees provide an interpretable structure that is beneficial for elucidating the reasoning behind the optimisation strategies of the converters. LSTM networks are specialised for their proficiency in time-series analysis, capturing the temporal correlations that are essential in wave energy predictions.

The addition of KPCA to LSTM networks (KPCA-LSTM) brings a novel dimension to the modelling toolkit. KPCA's capability for feature extraction, particularly in identifying non-linear patterns, complements LSTM's strength in sequential data prediction. This synergy enhances the model's ability to capture the nuanced patterns and long-term dependencies found in wave energy data. When combined, KPCA-LSTM augments the predictive accuracy, offering a potent solution for handling the complex and multi-faceted nature of wave energy conversion with improved precision and reliability.

## TALOS WEC POWER GENERATION PREDICTION MODEL

### TALOS WEC model

Fig. 2 demonstrates the PTO structure of TALOS. The PTO system is composed of a heavy ball at the centre. Six dampers (PTOs) are used

to connect the outside hull and the ball inside. Due to the weight of the ball, the ball would have relative motions to the hull when the incoming wave hits the WEC. Hence, motions coming from different directions will cause tension and compression forces on the dampers.

TALOS numerical modelling is based on a full-sized physical model of the device (Sheng et al., 2022a). The incoming long-crest irregular wave is generated with an average 10s period. A total of 20 variables are monitored, including water surface elevation, surge motion, heave motion, pitch motion, PTO force in the x direction, PTO force in the z direction, PTO moment in the y direction, forces applied on six PTOs, electric power generated by six PTOs, and total power.

**Prediction algorithm selection**

Addressing the complexity of forecasting the output of a two-body (hull and ball) WEC system like TALOS, requires a nuanced understanding of both traditional and modern forecasting methodologies. Traditional forecasting methods, such as Autoregressive Integrated Moving Average (ARIMA) and Exponential Smoothing (ES), have been widely used for their simplicity and effectiveness in predicting linear time series data (Elsaraiti & Merabet, 2021; Pierre et al., 2023). However, the TALOS WEC system, characterized by its interaction between two bodies in a dynamic marine environment, presents a challenge that goes beyond the capabilities of linear prediction models. These traditional methods often fall short when dealing with the non-linear, multi-dimensional, and stochastic nature of wave energy data, where the relationship between input variables and power output can be highly complex and time dependent.

In contrast, ML-based methods like SVM, ANN, and LSTM networks offer a more sophisticated approach to capturing the intricate patterns inherent in wave energy conversion processes (Xiang et al., 2018). SVM, for example, can handle non-linear data effectively using kernel functions, but it may struggle with large-scale datasets and multi-dimensional inputs. ANNs are capable of modelling complex non-linear relationships through their layered structure, yet they often require extensive data for training and can be prone to overfitting.

Table 1 outlines the strengths and limitations of these forecasting methods in the context of predicting the power output of a two-body WEC system.

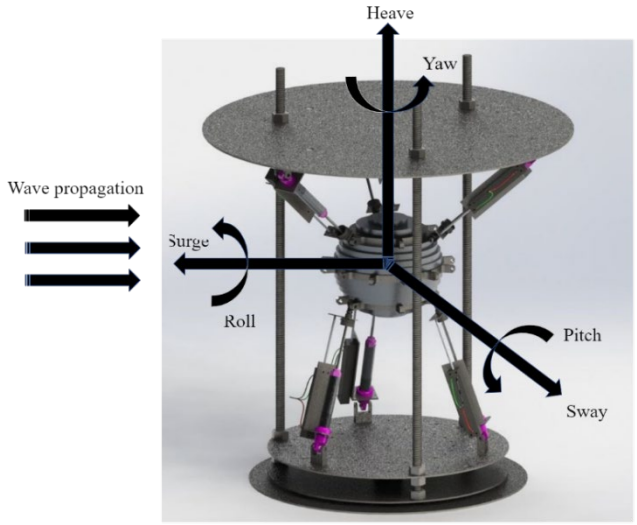


Fig. 2 TALOS II PTO system with six-degrees of freedom.

Table.1 Comparison of prediction algorithms.

| Method | Strengths | Limitations |
|---|---|---|
| ARIMA | Simple to implement.<br>Effective for linear series. | Struggles with non-linear data.<br>Limited in capturing long-term dependencies. |
| ES | Adapts well to data with trends and seasonality | Non-linear data challenges.<br>Limited complexity handling. |
| SVM | Handles non-linear data well.<br>Effective in high-dimensional spaces. | Scaling issues with large datasets<br>Limited interpretability. |
| ANN | Models complex non-linear relationships.<br>Adaptable to various types of data. | Requires extensive data for training.<br>Risk of overfitting. |
| LSTM | Excellent at learning long-term dependencies.<br>Effective for sequential, time-series data. | Computationally intensive.<br>Requires careful tuning of parameters. |

Given the TALOS WEC's operational complexity and the stochastic nature of wave energy, LSTMs stand out as the most robust method for forecasting its power output. Their ability to process and remember information over extended sequences, directly addresses the challenges posed by the dynamic and interdependent factors influencing WEC performance. Consequently, LSTMs offer a promising avenue for developing accurate and reliable predictive models for such advanced energy systems.

**LSTM**

The LSTM network consists of stacks of LSTM nets. The basic structure of the LSTM network is shown in Fig. 3 (Liu et al., 2019). One LSTM net includes input gates, forget gates, cell state, output gates, sigmoid gates, and tanh gates. Unlike other ML algorithms, LSTM emphasises the importance of the relationship between the previous and current states. The output of the current state is determined using the current input $X_t$ and the previous outputs, $h_{t-1}$ and $h_{t-2}$, i.e. the output from the previous states. The previous cell ($C_{t-1}$) and hidden state ($h_{t-1}$) are preserved and passed to the current cell state ($C_t$) and hidden state ($h_t$) without any losses. The sigmoid function ($\sigma$), which connects the previous states and current states, is used to decide which input data needs to be added or removed from the cell state. Thus, long-term dependency problems can be avoided.

To determine whether to keep or remove the input ($X_t$), the decision function of the forget gate ($f_t$) is used. The decision function ranges from 0 to 1, corresponding to the numbers in the cell state $C_{t-1}$, where the $W_f$ and $b_f$ are the weight and bias of the forget gate, respectively.

$$f_t = \sigma\left(W_f[h_{t-1}, X_t] + b_f\right) \quad (1)$$

Subsequently, the sigmoid function is employed to decide whether the new information needs to be preserved or forgotten. Contrasting with the sigmoid function, the *tanh* function is used to determine the importance of the information to be transmitted from the previous state. By multiplying the results from the sigmoid and *tanh* functions, the new current state $C_t$ is constructed from $C_{t-1}$, as follows,

$$i_t = \sigma(W_i[h_{t-1}, X_t] + b_i) \quad (2)$$
$$C_t = C_{t-1}f_t + tanh\,(W_n[h_{t-1}, X_t] + b_n)i_t \quad (3)$$

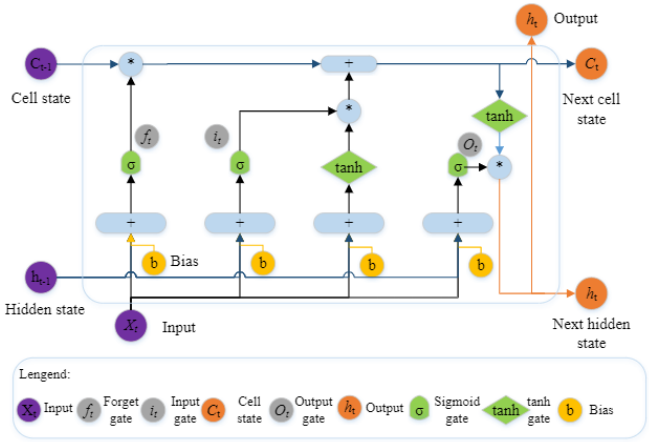


Fig. 3 LSTM structure.

The input gate $i_t$ is constructed from a sigmoid function calculated from the previous hidden state and input, where the $W_i$ and $b_i$ are the weight and bias of the input gate. The cell state $C_t$ is determined using the previous cell state $C_{t-1}$, forget gate $f_t$ and *tanh* function.

The output of the LSTM is computed from the hidden state ($h_t$) at the current time $t$ based on the output gate $O_t$,

$$O_t = \sigma\left(W_o[h_{t-1}, X_t] + b_o\right) \quad (4)$$

$$h_t = O_t tanh\left(C_t\right) \quad (5)$$

The output cell state is calculated from the sigmoid function of the previous hidden state $h_{t-1}$ and $X_t$, where $W_o$ and $b_o$ are the weight and bias of the output gate, respectively. The output hidden state is decided using the output gate $O_t$ and *tanh* function of the cell sate $C_t$.

LSTM networks are developed from RNNs (Recurrent Neural Networks). Thus, it has advantages in linking previous information to the current state, compared with other ML algorithms such as regression trees, SVR and ANN. Due to this characteristic, LSTM is suitable for regression modelling, for predicting and processing long-term time series data, as discussed by many researchers (Jalayer et al., 2021; Abdul et al., 2020; and Zhao et al., 2016).

**KPCA**

Kernel Principal Component Analysis (KPCA) is a multivariate statistical method. It extends traditional Principal Component Analysis (PCA) by employing a kernel function, allowing the originally linear operations to take place in a reproducing kernel Hilbert space (Abdi, 2010). PCA is a technique that transforms a group of correlated variables into a new set of linearly uncorrelated variables, termed principal components (PCs). It is a popular method for visualizing relationships and genetic distances between variables. This is typically achieved by calculating the eigenvalues of the data's covariance matrix or the singular values in cases of non-orthogonal matrix conditions. PCA is highly effective in reducing dimensions and has been validated across various research fields. By choosing the initial few PCs, the primary information is preserved while significantly reducing the dataset's dimensionality. Therefore, PCA is extensively used in feature extraction and integrated with ML algorithms like ANN, for applications such as monitoring and predicting wind turbine performance (Skittides, 2014 and Ata, 2015, Wang et al., 2016).

To extract PCs from a dataset $X$, eigen-analysis of the dataset's covariance matrix $\Sigma$ is performed. Initially, dataset $X$ is standardized:

$$Z_{ij} = \frac{x_{ij} - x_j}{\sigma_{x_j}} \qquad (i \neq j, i = j = 1,2,\dots,p) \quad (6)$$

where $x_j$ is the mean of $X_j$, $\sigma_{xj}$ is the standard deviation of $X_j$, and $Z$ is the standardized dataset $(Z_{ij})_{n\times p}$. The covariance matrix $\Sigma$ of $Z$ is:

$$\Sigma_{i,j} = cov\left(Z_i, Z_j\right) = E\left[\left(Z_i - \mu_i\right)\left(Z_j - \mu_j\right)\right] = E\left[Z_i Z_j\right] - \mu_i \mu_j \quad (7)$$

where $\mu_i = E(Z_i)$ is the mean of the $i$-th row vector in dataset $Z$. PCs are derived from the covariance matrix using singular value decomposition (SVD), where the singular values of $\Sigma$ are:

$$\Sigma = USW^T \quad (8)$$

Here, $S$ is an $n$-by-$p$ matrix containing the $i$-th singular values of $\Sigma$, $U$ is an $n$-by-$n$ matrix (the left singular vectors of $\Sigma$), and $W^T$ is a $p$-by-$p$ matrix (the right singular vectors of $\Sigma$). The $i$-th PC is obtained by:

$$Y_i = U_{i1}z_1 + U_{i2}z_2 + \cdots + U_{ip}z_p \qquad (i = 1,2,\dots,p) \quad (9)$$

The singular values of $\Sigma$ represent the variances of their corresponding PCs, indicating the weighted information from the original dataset. To choose the number of PCs, one calculates the cumulative variance contribution of each PC. The contribution of the $i$-th PC is:

$$\alpha_k = \frac{s_k}{\sum_{i=1}^{p} s_k} \quad (10)$$

where k is the number of PCs. To retain as much information from the original dataset as possible, $k$ should be as large as possible (k<n), but a balance must be found to achieve dimension reduction. Typically, the cumulative variance contribution is chosen to be no less than 85%.

**Power generation forecasting framework**

To operationalise the envisaged model, we adhere to a structured seven-step methodology, as depicted in the flowchart, Fig. 4. The initial stage involves the acquisition and preprocessing of time-series data, derived from the TALOS WEC numerical models cited in prior studies. The raw data, sampled at intervals of 0.05 seconds, encompasses 20 distinct monitoring variables, as described earlier (Sheng et al., 2022b). This stage segregates the data into training and testing subsets, with an additional focus on normalising the data. The causality inherent in the WEC system guides the selection of training inputs, which include water surface elevation, surge, heave, pitch motions, and the PTO forces along the x and z-axes, as well as the overall moment in the y-axis. These inputs are chosen based on their impact on the PTO forces, which are the primary forecasting target of the model. The model also considers the independence and potential interdependence of the six PTOs, accounting for scenarios where one PTO's failure could influence the dynamics of the others, thereby affecting the overall power output.

The dataset size, encompassing 12,000 data points with a 90% split for training and 10% for testing, is chosen to prevent overtraining and ensure robust learning without excessive computational demands. The subsequent stages, from the second to the fourth, focus on configuring the LSTM network parameters. This process is informed by previous successful applications and iterative testing with the same dataset, culminating in a set of optimised hyperparameters. These include a maximum of 250 epochs, a gradient threshold of 1, an initial learning rate of 0.05, a drop period of 125, and a drop factor of 0.2. Following the training phase, the model's precision is verified using the remaining 10% (1,200 points) of the dataset.

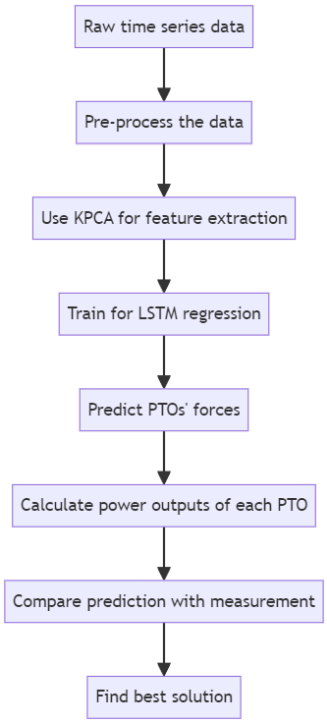


Fig. 4 TALOS WEC power generation model.

The architecture choice in the LSTM model is a strategic decision based on balancing the risks of underfitting and overfitting, and is based on our previous research (Wu & Ma, 2022).

The 3rd stage utilises Kernel Principal Component Analysis (KPCA) for feature extraction, enhancing the model's ability to capture complex patterns within the data. The prediction set is determined five time steps (0.25s) ahead toward the feature set. In the sixth step, the model is trained for LSTM regression, further refining its predictive capabilities with regard to PTO forces. Subsequent predictions of PTO forces lead to the seventh step, where the power output for each PTO is calculated. This facilitates a comparison between the model's predictions and actual measurements, aiding in the identification of the most accurate and efficient solution. The forces of the six PTOs are further used for the power outputs calculation, by using Eq. 11,

$$P = \frac{F^2}{\lambda} \tag{11}$$

where $P$ and $F$ are the power output and force of one PTO and $\lambda$ = 250,000 is the power coefficient based on hydrodynamic modelling.

Finally, the LSTM prediction accuracy is further compared with other machine learning algorithms. Both RMSE (root mean square error) in Eq. 12 and $R^2$ (coefficient of determination) in Eq. 13 are calculated to evaluate the forecasting model accuracy.

$$RMSE = \sqrt{\frac{\sum_{n=1}^{N}(\hat{y_n} - y_n)^2}{N}} \tag{12}$$

where $\hat{y}_n$ represents the prediction value and $y_n$ the measurement value. The RMSE value ranges from 0 to $+\infty$. Lower values indicate higher accuracy. $R^2$ is calculated as below:

$$R^2 = 1 - \frac{SS_{res}}{SS_{tot}} \tag{13}$$

where $SS_{res}$ and $SS_{tot}$ represent the residual sum of squares and total sum of squares, respectively. Normally, the $R^2$ value is ranges from 0 to 1, where 1 indicates the prediction model fits the data perfectly.

## POWER GENERATION RESULTS AND ANALYSIS

### PTO force predictions

Figures 5 and 6 show the KPCA-LSTM forecasting test results. In total, 1200 rows of data are used (10% of 12,000) for testing. Fig. 6 is a box plot representation that compares the distribution of predicted and measured values across six different PTO forces, while the Fig. 5 shows time-series plots for each PTO force, juxtaposing predicted and actual measurements over time.

The box plot provides a statistical summary that highlights the central tendency and dispersion of the predicted and measured values for each PTO. It is immediately apparent that the model's predictions are consistent with the measurements, given that the median of the predictions closely aligns with the median of the measurements across all PTO forces. However, there are notable differences in the interquartile ranges and the whiskers of the box plots, which suggest variability in the model's accuracy. The box plots for PTO forces 1, 5 and 6 indicate a wider range of variability in the predictions than in the measurements. In contrast, PTO forces 2, 3 and 4 show a closer match between the spread of predicted and measured data.

The time-series plots enable a more granular analysis of the model's performance. The oscillatory nature of the predicted and measured forces is evident and suggests a cyclic process. While the model captures the general trend and periodicity of the forces, there are instances where the predictions diverge from the measurements. These discrepancies might be due to the model's inability to fully account for the system's dynamic complexities or unexpected variations in the PTO forces that were not captured during the model training.

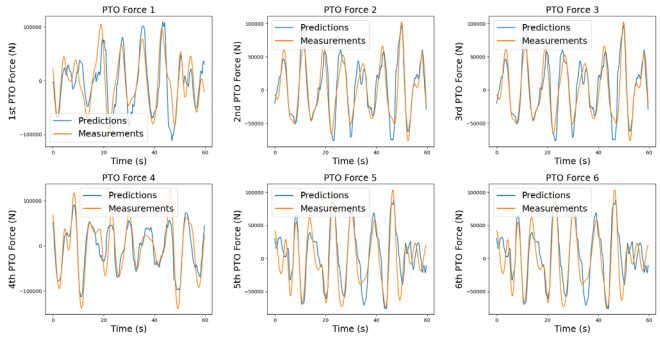


Fig. 5 TALOS WEC force prediction results.

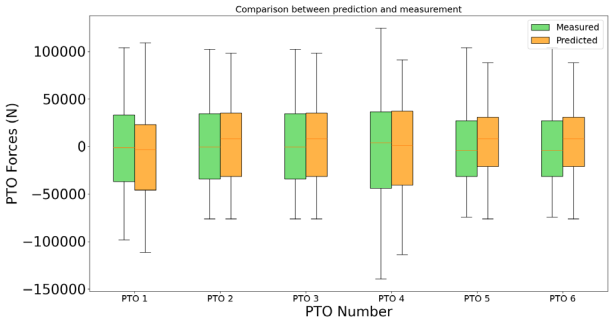


Fig. 6 Comparison between PTO force predictions and measurements.

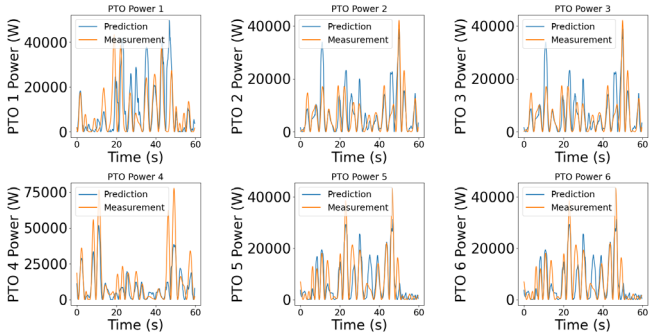


Fig. 7 TALOS WEC power prediction results.

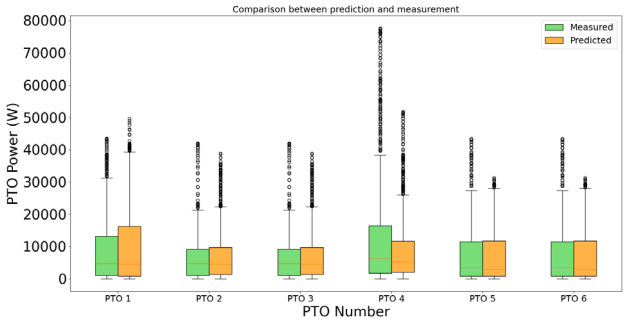


Fig. 8 PTO power predictions and measurements.

Analysis of these figures provides a nuanced perspective on the potential benefits of employing a KPCA-LSTM model for prediction. The KPCA-LSTM model's non-linear dimensionality reduction, coupled with its memory-capable architecture, may afford improvements in capturing the underlying patterns and reducing the prediction error. The current model's deviations, particularly the points where the predictions fail to align with the peaks and troughs of the measurements, could be addressed by the LSTM's ability to learn from long sequences of data and remember important information over extended time lags.

**PTO power predictions**

Fig. 7 presents a series of line graphs for six distinct PTO systems, comparing predicted and actual power outputs over time. This side-by-side portrayal facilitates a direct assessment of the predictive model's fidelity, revealing that the predictions adhere to the actual values to a variable extent. For PTO systems 1 and 4, there is a noteworthy degree of congruence between the predictions and actual measurements, despite occasional lapses in capturing peak values. Contrastingly, PTO systems 2, 3, 5 and 6 exhibit more marked divergences, especially in the accuracy and timing of predicted peaks.

Fig. 8 employs a boxplot to summarise the predictive and actual power values across all PTO systems. The visualisation elucidates the central tendencies and variances within the data, highlighting that, while median predicted values sometimes closely match the actual measurements, substantial variability is evident in other instances, as demarcated by the range of the interquartile spread and the outliers.

Scrutiny of these figures underscores specific aspects where the predictive model could be honed. The time-series line graphs indicate potential difficulties the model encounters with abrupt power fluctuations, as evidenced by the occasional missed peaks and troughs. The boxplot corroborates this by displaying a wider dispersion in predicted values relative to the measurements, implying inconsistencies in the model's ability to represent the data's true distribution. The integration of a KPCA-LSTM methodology has already advanced the precision of this model beyond that of traditional ANN, SVR, and standalone LSTM networks, especially given the complexity of the systems in question, which, when approached directly, have resulted in substantial prediction errors. Through KPCA, critical features that drive PTO power variability and sudden shifts are distilled. The LSTM networks are applied to these features to refine the prediction of temporal patterns.

Anticipated improvements from this advanced hybrid approach are multifaceted: it aims to heighten the accuracy in predicting peaks and to attenuate the discrepancy between the predicted and actual values. This should manifest as more constrained boxplot distributions that more accurately reflect the measured data. Furthermore, the enhanced capability for feature extraction and temporal prediction promises a model with not only improved accuracy but also heightened resilience to the dynamic changes in PTO power, which is crucial for real-world application reliability.

**Forecasting efficacy evaluation**

Accurate forecasting is paramount in the realm of wave energy conversion. Not only does it ensure optimal energy capture, safeguarding the maximisation of energy yields, but it also plays a foundational role in facilitating effective grid integration. By accurately forecasting power outputs, grid operators can adeptly manage energy inputs, ensuring a stable and reliable power supply. Moreover, precise predictions are instrumental in averting potential disturbances or grid imbalances that can arise from fluctuating energy inputs, especially given the inherently variable nature of wave energy.

In this landscape, the analysis of $R^2$ values emerges as a key metric. It offers a diagnostic lens, shedding light on the predictive prowess of the employed models, such as LSTM. As control systems of WECs rely heavily on these forecasts for real-time adjustments and operational decision-making, the pertinence of understanding the nuances of $R^2$ values cannot be overstated. Variations in these values across different forecast horizons can signal potential areas for model refinement, paving the way for more responsive and efficient control systems. A granular grasp of these dynamics ensures that WECs not only harness wave energy with heightened efficiency but also operate with enhanced predictability, optimising the symbiosis between power generation and control systems.

In the assessment of predictive modelling for WEC, the trajectory of the coefficient of determination $R^2$ across varying forecast intervals, as depicted in Fig. 11, offers a profound insight into the efficacy of simulation-based predictive models. The initial surge in $R^2$ is indicative of the model's high precision in short-term forecasting, which is paramount for the effective application of Model Predictive Control (MPC) strategies. This pronounced accuracy within the nascent stages of prediction underscores the model's capability to harness contemporaneous data and translate them into reliable force estimates for the PTO systems.

Conversely, the ensuing decline in $R^2$ upon extending the prediction window beyond the immediate horizon, accentuates the inherent limitations of the simulation model in encapsulating the complex, non-linear interactions within the marine environment. Such a decremental shift in predictive reliability suggests a divergence between the simulated projections and the system's nuanced response to evolving

hydrodynamic stimuli. This interval of diminished accuracy hints at the potential latency in the system's reaction to control inputs, due to physical constraints and the model's waning proficiency in forecasting under the rapidly shifting conditions that characterise wave dynamics.

Stabilisation of the $R^2$ metric in the subsequent phase reflects the model's recalibration to the broader, more persistent patterns of the simulated environment. This equilibrium suggests an alignment between the model's predictive capacity and the average behavioural tendencies of the wave energy system over extended periods, thus providing a consistent, albeit generalized, forecast that can inform longer-term strategic adjustments in the control and design of wave energy converters.

Such results, emanating from simulation data, highlight the critical importance of iterative model refinement and validation against a spectrum of temporal scales, to fine-tune the forecasting tools used within the wave energy sector. The simulated environment serves as a testbed for developing robust predictive algorithms that can anticipate and navigate the complexities of real-world wave energy conversion, thereby fostering advancements in control mechanisms and enhancing the overall efficacy of energy harnessing from oceanic waves.

**Power output forecasting accuracy comparison**

Table 2 presents a comparative analysis of the prediction accuracy across five distinct algorithms, delineating the overall $R^2$ and RMSE values for the power output prediction of six PTOs. A close examination of the table reveals that the LSTM algorithm exhibits commendable performance, often surpassing the other models in overall prediction accuracy. Notably, for the 2nd and 5th PTOs, the LSTM algorithm achieves the highest $R^2$ values, underscoring its superior predictive capabilities. The KPCA-LSTM model, which integrates kernel KPCA with the LSTM framework, shows strong performance, particularly in the $R^2$ values for the 2nd, 3rd, and 5th PTOs, where it outperforms the standalone LSTM. This suggests that the KPCA preprocessing step effectively captures relevant features from the input data, enhancing the LSTM's ability to model complex relationships.

For the 2nd PTO's power prediction, the SVR model yields the lowest RMSE, indicating a slightly better prediction precision for this particular PTO compared to the LSTM. In the case of the 1st PTO, however, the SVR and LSTM are equally accurate, both achieving the lowest RMSE of 0.12. The regression tree, with its simpler structure, demonstrates the weakest performance in both metrics across all PTOs, suggesting that the complexity of the LSTM and KPCA-LSTM models may contribute to their heightened accuracy. Finally, the SVR and ANN (multilayer perceptron) models exhibit similar performance levels, slightly trailing behind the LSTM.

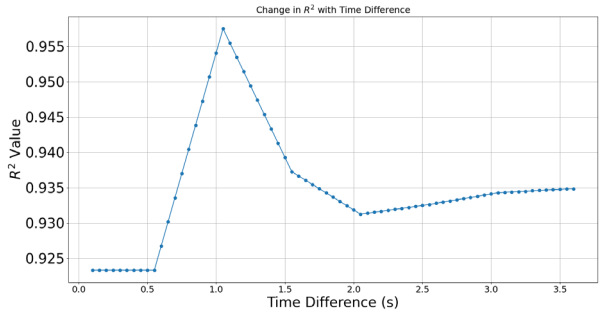


Fig. 11 Changes of $R^2$ values with increasing forecast time for the sixth PTO forces.

Table 2. Prediction accuracy of five algorithms (RT: Regression tree).

| PTO | $R^2$ or RMSE | KPCA-LSTM | LSTM | RT | SVR | ANN |
|---|---|---|---|---|---|---|
| 1st | $R^2$ | 0.87 | 0.67 | 0.44 | 0.78 | 0.56 |
| 2nd | $R^2$ | 0.93 | 0.49 | 0.56 | 0.67 | 0.45 |
| 3rd | $R^2$ | 0.92 | 0.83 | 0.75 | 0.74 | 0.78 |
| 4th | $R^2$ | 0.89 | 0.93 | 0.74 | 0.74 | 0.77 |
| 5th | $R^2$ | 0.85 | 0.92 | 0.52 | 0.81 | 0.83 |
| 6th | $R^2$ | 0.92 | 0.92 | 0.79 | 0.89 | 0.80 |
| 1st | RMSE | 0.12 | 0.13 | 0.17 | 0.13 | 0.16 |
| 2nd | RMSE | 0.08 | 0.15 | 0.16 | 0.14 | 0.17 |
| 3rd | RMSE | 0.09 | 0.11 | 0.14 | 0.13 | 0.13 |
| 4th | RMSE | 0.11 | 0.08 | 0.13 | 0.13 | 0.13 |
| 5th | RMSE | 0.12 | 0.09 | 0.13 | 0.12 | 0.12 |
| 6th | RMSE | 0.09 | 0.09 | 0.13 | 0.11 | 0.12 |

## CONCLUSIONS

This article has compared a novel KPCA-LSTM approach with several other ML approaches for the prediction of power generation from a multi-DOF WEC presently in development. The work is presently limited to the analysis of simulated data. It is concluded from the results that KPCA-LSTM offers a feasible approach for such power generation forecasting. Based on evaluation results of $R^2$ and RMSE, the KPCA-LSTM algorithm yields improved performance compared to several other, more conventional ML algorithms. With the development of power prediction methods, better design of WEC control systems and power management becomes feasible, especially for offshore power management.

Theoretically, the LSTM network bypasses the intricate physical interdependencies inherent in a two-body wave energy converter system. Instead, it focuses directly on predicting the output based on historical input data. By doing so, the LSTM leverages its strength in pattern recognition from time-series data, effectively making forecasts without delving into the complex physics of the system's interactions. This approach allows for efficient prediction while circumventing the need for detailed modelling of the system's physical dynamics.

The current work on hyperparameter selection for LSTM networks is based on prior knowledge and commonly used parameters. In other words, it selects hyperparameters manually, which might cause extra errors in the prediction. The next steps will consider algorithm optimisation work related to hyperparameter selection for the training model, and investigations into other potential algorithms suitable for power prediction in this multi-DOF WEC context.

## ACKNOWLEDGEMENTS

This work was supported by the EPSRC, Grant number EP/V040561/1, UK, for the project Novel High-Performance Wave Energy Converters with advanced control, reliability, and survivability systems through machine-learning forecasting (NHP-WEC).

## REFERENCES

Abdul, Z.K., Al-Talabani, A.K., & Ramadan, D.O. (2020). A hybrid temporal feature for gear fault diagnosis using the long short-term memory. *IEEE Sensors Journal*, 20(23), 14444-14452.

Abdi, H., & Williams, L. J. (2010). Principal component analysis. *Wiley Interdisciplinary Reviews: Computational Statistics*, 2(4), 433-459. doi:10.1002/wics.101.

Aggidis, G.A., & Taylor, C.J. (2017). Overview of wave energy converter devices and the development of a new multi-axis laboratory prototype. In 20th IFAC Triennial World Congress, 9–14 July, Toulouse, France. Elsevier, *IFAC–PapersOnLine*, 50(1), 15651–15656.

AquaBuOy. (2016). *Finavera aquabuoy*. http://www.global-greenhousewarming.com/Finavera-aquabuoy.html

Arulkumaran, K., Deisenroth, M. P., Brundage, M., & Bharath, A. A. (2017). Deep reinforcement learning: A brief survey. IEEE Signal Processing Magazine, 34(6), 26-38.

Ata, R. (2015). Artificial neural networks applications in wind energy systems: a review. *Renewable and Sustainable Energy Reviews*, 49, 534-562.

AWS Ocean. (2016). Archimedes Waveswing submerged wave power buoy. http://awsocean.com/technology/archimedeswaveswing-submerged-wave-power-buoy

Benbouzid, M., Berghout, T., Sarma, N., Djurović, S., Wu, Y., & Ma, X. (2021). Intelligent condition monitoring of wind power systems: State of the art review. *Energies*, 14(18), 5967.

Bento, P.M.R., Pombo, J.A.N., Mendes, R.P.G., Calado, M.R.A., & Mariano, S.J.P.S. (2021). Ocean wave energy forecasting using optimised deep learning neural networks. *Ocean Engineering*, 219, 108372.

Bhatt, J., Carthy, J., Clark, T., Galea, S., Sutch, A., Tutt, A., & Walker, J. (2016). Optimisation and development of a multi-axis wave energy converter device (Master of Engineering Project Report). Engineering Department, Lancaster University.

Boyle, G., & Duckers, L. (2012). Renewable energy: Power for a sustainable future. OUP Oxford.

Cunningham, P., Cord, M., & Delany, S. J. (2008). *Supervised learning. In Machine learning techniques for multimedia: case studies on organization and retrieval* (pp. 21-49). Berlin, Heidelberg: Springer Berlin Heidelberg.

Darwish, A., & Aggidis, G.A. (2022). A review on power electronic topologies and control for wave energy converters. *Energies*, 15(23), 9174.

Desouky, M.A., & Abdelkhalik, O. (2019). Wave prediction using wave rider position measurements and NARX network in wave energy conversion. *Applied Ocean Research*, 82, 10-21.

Elsaraiti, M.; Merabet, A. (2021). A Comparative Analysis of the ARIMA and LSTM Predictive Models and Their Effectiveness for Predicting Wind Speed. *Energies*, *14*, 6782.

Jalayer, M., Orsenigo, C., & Vercellis, C. (2021). Fault detection and diagnosis for rotating machinery: A model based on convolutional LSTM, Fast Fourier and continuous wavelet transforms. *Computers in Industry*, 125, 103378.

Joseph, K., Sharma, A. K., & Van Staden, R. (2022). Development of an intelligent urban water network system. *Water*, 14(9), 1320.

Li, G., Weiss, G., Mueller, M., Townley, S., & Belmont, M.R. (2012). Wave energy converter control by wave prediction and dynamic programming. *Renewable Energy*, 48, 392-403.

Liu, Y., Guan, L., Hou, C., Han, H., Liu, Z., Sun, Y., & Zheng, M. (2019). Wind power short-term prediction based on LSTM and discrete wavelet transform. *Applied Sciences*, 9(6), 1108.

Liu, Z., Wang, Y., & Hua, X. (2020). Prediction and optimization of oscillating wave surge converter using machine learning techniques. *Energy Conversion and Management*, 210, 112677.

McCabe, A.P., Bradshaw, A., Meadowcroft, J.A., & Aggidis, G. (2006). Developments in the design of the PS Frog Mk 5 wave energy converter. *Renewable Energy*, 31, 141–151.

Mousavi, S. M., Ghasemi, M., Dehghan Manshadi, M., & Mosavi, A. (2021). Deep Learning for Wave Energy Converter Modeling Using Long Short-Term Memory. *Mathematics*, 9(8), 871.

Ni, C., Ma, X., & Bai, Y. (2018, September). Convolutional Neural Network based power generation prediction of wave energy converter. *In 2018 24th International Conference on Automation and Computing (ICAC)* (pp. 1-6). IEEE.

Orecon. (2009). Renewable Energy Focus, Wave energy developer Orecon hits stormy waters. http://www.renewableenergyfocus.com/view/5700/wave-energy-developer-orecon-hits-stormy-waters

Peña-Sánchez, Y., García-Abril, M., Paparella, F., & Ringwood, J. V. (2018). Estimation and forecasting of excitation force for arrays of wave energy devices. *IEEE Transactions on Sustainable Energy*, 9(4), 1672-1680.

Pierre, A.A.; Akim, S.A.; Semenyo, A.K.; Babiga, B. (2023). Peak Electrical Energy Consumption Prediction by ARIMA, LSTM, GRU, ARIMA-LSTM and ARIMA-GRU Approaches. *Energies*, *16*, 4739.

Powerbuoy. (2016). Ocean Power Technologies. http://www.oceanpowertechnologies.com/powerbuoytechnology

Reikard, G., Robertson, B., & Bidlot, J. R. (2015). Combining wave energy with wind and solar: Short-term forecasting. *Renewable Energy*, 81, 442-456. https://doi.org/10.1016/j.renene.2015.03.016

Salter, S. H. (1974). Wave Power. *Nature*, 249, 720–724.

Sheng, W., Tapoglou, E., Ma, X., Taylor, C. J., Dorrell, R. M., Parsons, D. R., & Aggidis, G. (2022a). Hydrodynamic studies of floating structures: Comparison of wave-structure interaction modelling. *Ocean Engineering,* 249, 110878.

Sheng, W., Tapoglou, E., Ma, X., Taylor, C. J., Dorrell, R., Parsons, D. R., & Aggidis, G. (2022b). Time-Domain Implementation and Analyses of Multi-Motion Modes of Floating Structures. *Journal of Marine Science and Engineering*, 10(5), 662.

Skittides, C., & Fruh, W. G. (2014). Wind forecasting using principal component analysis. *Renewable Energy*, 69, 365-374.

Taylor, C. J., Bradshaw, A., Chaplin, R. V., French, M., & Widden, M. B. (2002). Wave Energy Research at Lancaster University: PS FRog and Frond. *World Renewable Energy Congress VII*, Cologne, Germany.

Wave power firm Pelamis calls in administrators. (2014, November 21). *BBC News*. http://www.bbc.co.uk/news/uk-scotland-scotland-business-30151276

Wave Hub. (2016). Carnegie Wave Energy Limited. http://www.wavehub.co.uk/wave-hub-site/ourcustomers/carnegie-wave-energy-limited

Wang, Y. (2020). Predicting absorbed power of a wave energy converter in a nonlinear mixed sea. *Renewable Energy*, 153, 362-374.

Wang, Y., Ma, X. And Joyce, M. (2015). Reducing sensor complexity for monitoring wind turbine performance using principal component analysis. *Renewable Energy,* 97, 444-456.

Wu, Y., & Ma, X. (2022). A hybrid LSTM-KLD approach to condition monitoring of operational wind turbines. *Renewable Energy*, 181, 554-566.

Xiang, Y., Gou, L., He, L., Xia, S., & Wang, W. (2018). A SVR–ANN combined model based on ensemble EMD for rainfall prediction. *Applied Soft Computing*, 73, 874-883.

Yürüşen, N. Y., Uzunoğlu, B., Talayero, A. P., & Estopiñán, A. L. (2021). Apriori and K-Means algorithms of machine learning for spatio-temporal solar generation balancing. Renewable Energy, 175, 702-717.

Zhang, J., Zhao, X., Jin, S., & Greaves, D. (2022). Phase-resolved real-time ocean wave prediction with quantified uncertainty based on variational Bayesian machine learning. *Applied Energy*, 324, 119711.

Zhao, R., Wang, J., Yan, R., & Mao, K. (2016, November). Machine health monitoring with LSTM networks. *In 2016 10th International Conference on Sensing Technology (ICST)* (pp. 1-6). IEEE.

Zou, S., Zhou, X., Khan, I., Weaver, W. W., & Rahman, S. (2022). Optimization of the electricity generation of a wave energy converter using deep reinforcement learning. *Ocean Engineering*, 244, 110363.